RASĀYAN *J. Chem.*
Vol. 15 | No. 3 |2171-2180| July - September | 2022
ISSN: 0974-1496 | e-ISSN: 0976-0083 | CODEN: RJCABP
http://www.rasayanjournal.com
http://www.rasayanjournal.co.in

STRUCTURAL, OPTICAL, AND PARAMAGNETIC INVESTIGATIONS OF (Mn^{2+}) IONS DOPED ZINCALUMINOBOROPHOSPHATE (ZnAlBP) GLASS SYSTEM

J. Suresh Krishna[1], S. Hima Bindu[2], D. Siva Raju[1,3], M. Hema Latha[1], V. Vinay Krishna[4] and Ch. Linga Raju[1,✉]

[1]Department of Physics, Acharya Nagarjuna University, Guntur-522510, (AP) India
[2]Department of Physics, National Institute of Technology, Warangal-506004, (Telangana) India
[3]Department of Physics, Indian Institute of Science Education and Research, Tirupati-517507, (AP) India
[4]Department of Electronics & Instrumentation Technology, Acharya Nagarjuna University, Guntur-522510, (AP) India
✉Corresponding Author: drchlraj_phy@yahoo.com

ABSTRACT

Concentration variation of Mn^{2+} ions doped zincaluminoborophosphate (ZnAlBP) glasses of 40 ZnO + 25 H_3BO_3 + (30-x) P_2O_5 + 5 Al_2O_3 + x MnO with $0 \le x \le 0.8$ (x=0, 0.2, 0.4, 0.6 and 0.8) have been prepared and investigated by structural and spectroscopic techniques. The XRD diffractograms confirm the amorphous nature of the prepared samples. The FTIR spectra reveal the existence of BO_3 and BO_4 units along with fundamental P-O-H and B-O-H structural units in the present glass system. The Optical absorption spectra exhibit two low intensity bands centered at 407 nm (24,570 cm^{-1}) and 689 (14,514 cm^{-1}). These bands were assigned to $^6A_{1g}(S) \rightarrow {}^4A_{1g}(G) + {}^4E_g(G)$ and $^6A_{1g}(S) \rightarrow {}^4T_{1g}(G)$ characteristic transitions of Mn^{2+} ions in octahedral symmetry. Tauc's plots were drawn to measure the optical band gaps for the direct and indirect transitions. The energy gaps show a decreasing trend for the selected ZnAlBP: Mn^{2+} glass system. The well-resolved hyperfine splitting EPR spectra of prepared glass samples exhibit resonance at $g \approx 1.98$ indicating the Mn^{2+} ions are in octahedral site symmetry. The hyperfine splitting factor (hfs), the number of spin levels (N), hyperfine constant (A), zero-field splitting parameter (D), and paramagnetic susceptibility (χ) have been determined. The magnitude of g indicates the predominant ionicity in the glasses.

Keywords: Glasses, Band Gaps, Optical Basicity, Octahedral Symmetry, g-Factor, Ionicity.

RASĀYAN*J. Chem.*, Vol. 15, No.3, 2022

INTRODUCTION

ZnO is an extensively used additive to the phosphate network to improve chemical durability.[1]ZnO in a phosphate network can have better physical properties including chemical durability. Oxide glasses are the key materials in industrial applications due to their high transparency, wide composition, simple fabrication, and good glass forming ability.[2]Glasses containing transition metal (TM) ions have grabbed more interestbecause oftheir versatile properties in electrical, magnetic, and optical properties with applications like memory devices, storage devices, etc.[3] Borophosphate glasses are favorable materials for optical applications due totheir superior optical properties, low refractive indices, and dispersion and good transparency from the UV to the NIR regions.[4] Borate glasses are identified to be a functional material in dosimetry applications considering the fact that their effective atomic number is close to that of human tissue.[5,6,7] The Mn^{2+} ion can exhibit both octahedral and tetrahedral symmetry when introduced into glass hosts. The manganese ions are prominent paramagnetic ions when existing in Mn^{2+} and Mn^{3+} states and luminescent activators in Mn^{2+} and Mn^{4+} states.[8] The glasses doped with TM ions have attracted good attention due to their unique potential applications as solid-state lasers, phosphor materials, photo devices, magnetic materials, etc.[9]The salient features of these glasses are highly useful in optical industries such as switches, isolators, and IR Windows.[10] Substitution of alkali metals into oxide glass host modifies the glass network which leads to the variations in properties.[11,12]

http://doi.org/10.31788/RJC.2022.1536992

The present EPR investigations reveal the organization of manganese ions in ZnAlBP oxide glasses can exist in Mn^{2+} with octahedral site symmetry.[13]The present glasses can have two groups of bands one is due to trigonal BO_3 units and the other is due to the tetrahedral BO_4 units.[14] Many researchers proved that the ratio of B_2O_3/Al_2O_3 greatly influences the glass transition temperature and also the incorporation of Al_2O_3 into the borate or silicate glass network may exist in AlO_4 structural units.[15] Furthermore, borophosphate glasses are suitable to host materials for the optical industry due to enormous optical properties such as low refractive index and dispersion, and high transparency from UV to NIR regions.[16,17,18] The greater solubility of TM ions in the phosphate glass is a key parameter over the other glasses hosts and manganese ions have greater optical, electrical, and magnetic properties.[19,20] In the current work, the authors studied and investigated the Mn^{2+} ions doped zincaluminoborophosphate (ZnAlBP) glasses using UV-Vis, EPR, and FTIR techniques.

EXPERIMENTAL

Material and Methods

The Mn^{2+} ions doped zincaluminoborophosphate (ZnAlBP) glass system of 40 ZnO + 25 H_3BO_3 + (30-x) P_2O_5 + 5 Al_2O_3 + x MnO with $0 \le x \le 0.8$ (x=0, 0.2, 0.4, 0.6 and 0.8) have been synthesized by melt quenching technique. These glasses are synthesized by grinding the chemicals ZnO, H_3BO_3, P_2O_5, Al_2O_3, and $MnCO_3$ in appropriate quantities and collecting the obtained homogeneous mixture into a silica crucible. Now carefully place the crucible into the programmable furnace and heat it up to 1250 °C for 2 hours. The resultant melt was quickly compressed with another plate by pouring it onto a heated brass plate.Now the obtained glass samples were annealed for 3 hours at 430 °C to avoid thermal strains. The density of the titled glasses is calculated by adopting the Archimedes principle. The refractive index is measured using Abbe's refractometer. The crystallinity of the present samples was examined by XRD studies. The structural analysis was performed with FTIR studies. The optical absorption spectra of the glass samples were measured using a UV-Vis spectrophotometer (JASCO-V670) at a wavelength of 400- 800 nm. The EPR spectra of the glasses were measured using an EPR spectrometer (JEOL-JESFA 200). The detailed chemical compositions of the ZnAlBP and Mn^{2+} doped ZnAlBP glass are depicted in table-1 and the photograph of the sample is shown in Fig.-1.

Fig.-1: A Photograph of ZnAlBP: Mn^{2+} (Pure, 0.2, 0.4, 0.6 and 0.8) Glasses

Table-1: Chemical Composition of ZnAlBP and Mn^{2+} doped ZnAlBP Glass System

Glass code	Glass constituents (in wt %)				
	ZnO	H_3BO_3	P_2O_5	Al_2O_3	MnO
ZnAlBP	40	25	30	5	---
ZnAlBP: Mn(0.2)	40	25	29.8	5	0.2
ZnAlBP: Mn(0.4)	40	25	29.6	5	0.4
ZnAlBP: Mn(0.6)	40	25	29.4	5	0.6
ZnAlBP: Mn(0.8)	40	25	29.2	5	0.8

RESULTS AND DISCUSSION

Physical Parameters

The physical parameters will play a vital role in the determination of structural changes that occurred during the preparation of samples. The physical parameters were determined using the standard formulas[21] and are reported in table-2. The mass density of the glasses decreases from 3.407 to 3.028 g/cm^3 with an increase in MnO ion concentration. The reason for the decrement in density may be due to the replacement of higher molar mass phosphate (141.94 g/mol) with lower molar mass manganese (70.93

g/mol). The obtained changes in density were an indication of structural changes in the glass matrix during synthesis. The average molecular weight varied from 95.635 to 95.067 g/mol with dopant concentration and it could be due to the lower molar mass of MnO than P_2O_5. The molar volume of the glass system changes from 28.070 to 31.395 cm^3/mol, because the trend of the molar volume is opposite to the density.[22] Transition metal ion concentration increases from 4.175 to 15.34 x 10^{21} ions/cm^3 with TM ion content from 0.2 to 0.8 wt%, which in expected result. The polaron radius and internuclear distance are found to be decreased from 2.502 to 1.662 Å and 6.210 to 4.024 Å with MnO concentration from 0.2 to 0.8 wt%. The increase in dopant concentration leads to a decrease in free space, resultingin the more compactness ofthe glass structure. The magnitude of field strength varied from 3.194 to 7.611 x 10^{15} cm^{-2} with selected MnO content and it may be because of the strong bond strength between Mn-O and higher field strengths around Mn^{2+} ion at higher concentrations.[23] The magnitude of refractive index (RI) is directly proportional to the availability of non-bridging oxygens (NBOs) having high polarizability than bridging oxygens (BOs). The obtained values of refractive indices are ranging from 1.618 to 1.623 and the authors noticed that the Mn 0.4 % hasa high refractive index due to the availability of more NBOs for this concentration. The switching of TM ions in the phosphate glass network may cause the breaking of the P-O-P links and accumulate a large number of NBOs.[24] The measured metallization values are useful for conducting the nature of the prepared samples. The trends of dielectric and optical dielectric constant values were observed to be increasing to Mn 0.4 % and thereafter decreased to Mn 0.8% because the quantities are directly proportional to the refractive index. The higher magnitudes of molar refractivity (23.801 cm^3) and polarizability (9.435 x 10^{-24} cm^3) for Mn 0.4 % are mainly due to the availability of a greater number of NBOs.[21] The observed trends and those previously reported for Mn^{2+} doped phosphate-based glass systems are in good accord.

X-ray Diffraction Studies

The XRD pattern of the ZnAlBP and Mn^{2+} doped ZnAlBP samples were recorded in the range of $10^o < 2\theta < 80^o$. The recorded spectra of the different dopant ion compositions i.e., ZnAlBP, ZnAlBP: Mn(0.2), ZnAlBP: Mn(0.4), ZnAlBP: Mn(0.6) and ZnAlBP: Mn(0.8) are shown Fig.-2. In the present glass system, the XRD diffractograms consist of only one single broad hump centered at $2\theta=28^o$ and no other sharp peaks were identified which confirms the amorphous/ glassy nature of the prepared samples.[25]

Functional Group (FTIR) Studies

The FTIR spectra of ZnAlBP and Mn^{2+} doped ZnAlBP glasses are depicted in Fig.-3. The FTIR spectra consist of several bands identified from 4000-400 cm^{-1}. The obtained bands and band positions are shown in table-3. The bands at 3755-3776 cm^{-1} are assigned to O-H bonds which may be attributed to the possible moisture absorption. The O-H vibrations are increased with the manganese content the trend might be due to the breaking of bonds. The symmetric stretching vibrations of water OH or P-O-H and B-O-H are assigned to the bands at 2930-1750 cm^{-1}, indicating the hygroscopic nature of the glasses.

Table- 2: Physical Parameters of ZnAlBP and Mn^{2+} doped ZnAlBP Glasses

Physical and optical parameters	ZnAlBP	ZnAlBP			
		Mn(0.2)	Mn(0.4)	Mn(0.6)	Mn(0.8)
Thickness (t), cm	0.323	0.333	0.318	0.321	0.312
Density (ρ), cm^3	3.407	3.310	3.201	3.104	3.028
Avg. molecular weight (M_i), g/mol	95.635	95.493	95.351	95.209	95.067
Molar volume (V_M), cm^3/mol	28.070	28.849	29.787	30.673	31.395
TM ion concen. (N_{TM} x10^{21}), ions/cm^3	0	4.175	8.087	11.781	15.347
Polaron radius (r_p), Å	0	2.502	2.007	1.770	1.6621
Inter nuclear distance (r_i), Å	0	6.210	4.982	4.394	4.024
Field strength (F x 10^{15}), cm^{-2}	0	3.194	4.965	6.380	7.611
Refractive index (n)	1.618	1.619	1.623	1.622	1.621
Dielectric constant (ε)	2.617	2.621	2.634	2.630	2.627
Optical dielectric constant (?)	1.617	1.621	1.634	1.630	1.627
Reflection loss (R), %	5.572	5.586	5.641	5.627	5.613
Molar refractivity (R_M), cm^3	23.777	23.774	23.801	23.653	23.552
Ele. polarizability (α_e x 10^{-24}), cm^3	9.426	9.424	9.435	9.376	9.336
Metallization (M)	0.152	0.175	0.201	0.229	0.249
Reflection factor (P)	0.894	0.894	0.895	0.893	0.893
Electrical susceptibility (χ)	0.208	0.208	0.209	0.209	0.209

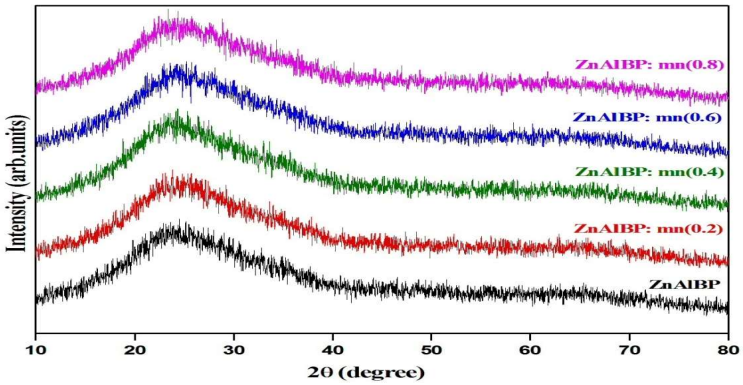

Fig.-2: XRD Diffractograms of ZnAlBP and Mn^{2+} doped ZnAlBP Glasses

The asymmetric and symmetric stretching vibrations of P-O-P groups and the B-O stretching vibrations of BO_4 units in Penta borate groups, give rise to BPO_4 and B-O-P units,[26,27]which causes the band at 1048 cm^{-1} and 846 cm^{-1}. The peak of 759 cm^{-1} is attributed to the symmetric stretching vibrations of the phosphate tetrahedron's bridging oxygens (BOs) bound to phosphate (P-O-P).These bands are due to vibrations of B-O-B linkages of BO_3 and BO_4 units. The low intense band identified at 509 and 536 cm^{-1} is ascribed to ZnO_4 and MnO_4 units.[28]

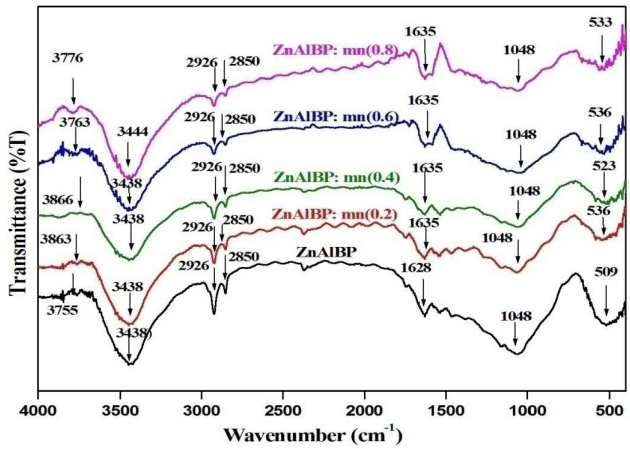

Fig.-3: FTIR Spectra of ZnAlBP and Mn^{2+} Doped ZnAlBP Glasses

Table-3: FTIR Bands and Their Assignments of ZnAlBP and Mn^{2+} Doped ZnAlBP Glasses

ZnAlBP	ZnAlBP				Bands Assignment
	Mn(0.2)	Mn(0.4)	Mn(0.6)	Mn(0.6)	
509	536	523	536	533	meta-centres for ZnO_4 and MnO_6units
767	774	759	779	761	BO_3 and BO_4units
839	846	837	842	846	$(B\text{-}O\text{-}P)_{st}$ and $(P\text{-}O\text{-}B)_{st}$
1048	1048	1048	1048	1048	$(P\text{-}O\text{-}P)_{asy}$ group (PO_4^{3-}) units
1628	1635	1635	1635	1635	H-O-H bending vibrations
2850	2850	2850	2850	2850	OH (or) $(P\text{-}O\text{-}H)_{st}$, $(B\text{-}O\text{-}H)_{st}$
2926	2926	2926	2926	2926	OH (or) $(P\text{-}O\text{-}H)_{st}$, $(B\text{-}O\text{-}H)_{st}$
3438	3438	3438	3438	3444	O-H stretching vibrations
3755	3863	3866	3736	3776	Stretching vibrations of H_2O

Optical Absorption Studies

The UV-Vis spectra of selected concentrations of Mn^{2+} doped ZnAlBP glasses are shown in Fig.-4. The absorption spectra of the glasses have been recorded in the wavelength region of 400-800 nm at room temperature. In glasses, the manganese in $Mn^{2+}(d^5)$ state can exist in both the tetra and octahedral

environments with free ion terms ^6S, ^4P, ^4F, and^4G. The absorption spectra of the selected glass system exhibit three less intense bands centered at 480 nm (20,833 cm^{-1}), 526 nm (19, 011 cm^{-1}), and 690 nm (14,493 cm^{-1}) are assigned to the transitions $^5E_g \rightarrow {}^5T_{2g}$, $^6A_{1g}(S) \rightarrow {}^4T_{2g}(G)$ and $^6A_{1g}(S) \rightarrow {}^4T_{1g}(G)$ respectively which represents the characteristic absorption of distorted octahedral site symmetry of Mn^{2+} ion.[29-31]The quartet states ^4G, ^4F, and ^4P are located above the ground state (^6S) in the octahedral crystal field, and the trigonal CF divides the four levels into 10 sublevels. Due to the spin-forbidden transitions from the ground state (^6S) to the excited levels, as well as the $3d^5$ shape of the Mn^{2+} ion, there are few optical absorption lines of Mn^{2+}. According to Hund's rule the manganese has a ground state of $^6A_{1g}$ octahedral symmetry. The optical spectra of Mn^{2+} ions possess only spin forbidden transitions due to excited states of the Mn^{2+} ion (d^5 configuration). The band around 690 nm is ascribed to the transition $^6A_{1g}$ (S) $\rightarrow {}^4T_{1g}$ (G) which depends on Dq. The optical transitions are specified by using Tanabe-Sugano diagram.[32,33]

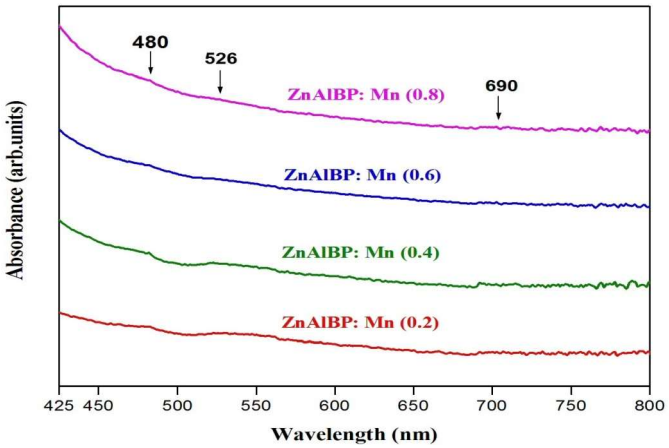

Fig.-4: UV-Vis Spectra of Mn^{2+} Doped ZnAlBP Glasses

Optical Basicity (Λ_{th}), Band Gap (E_{opt}), and Urbach Energy (ΔE)

In oxide glasses, optical basicity is one of the major parameters and it can be measured regarding the ability to contribute negative charge to the ion.[34] The magnitude of Λ_{th} of the glass can be evaluated using the standard formula.[35] It was noticed that the optical basicity of the glasses decreases with an increase in the dopant (Mn^{2+}) content and a similar trend was observed in the other glass materials reported for manganese ion. [35,36] In amorphous materials, the optical band gap is considered to be as the energy gap between the valance and conduction band.[36,37] Tauc's plots were drawn to evaluate the band gaps by plotting $(\alpha h\nu)^2$ and $(\alpha h\nu)^{1/2}$ as a function of photon energy ($h\nu$) as shown in Fig.-5(a) and (b) respectively.

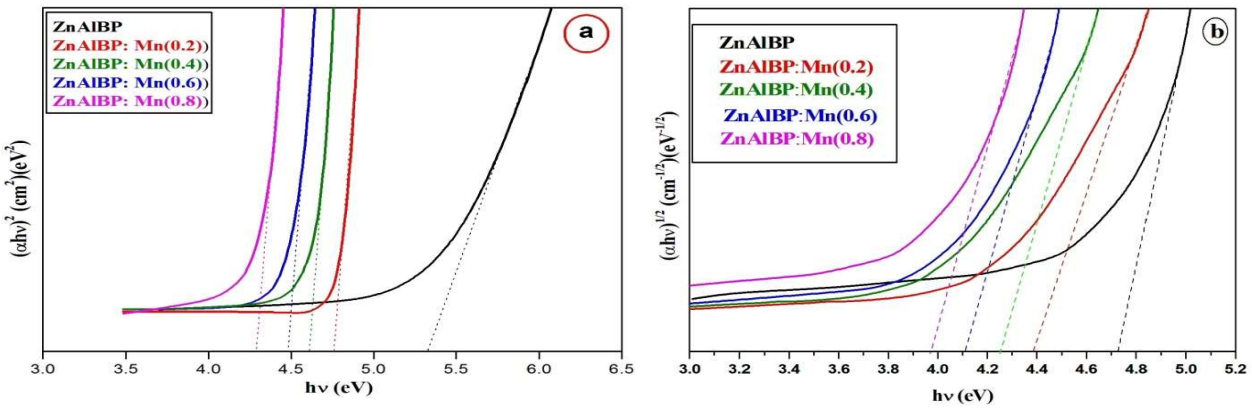

Fig.-5: Tauc Plots of (a) Direct and (b) Indirect Band gaps of ZnAlBP and Mn^{2+} Doped ZnAlBP Glasses

Table- 4: The bandgaps, Urbach Energies, and Optical Basicity of ZnAlBP and Mn^{2+} doped ZnAlBP Glasses

Sample Code	Band Gap (eV)		UrbachEnergy ΔE (eV)	Optical Basicity (Λ_{th})	Ref.
	Direct	Indirect			
ZnAlBP	5.31	4.73	0.178	0.7604	Present work
ZnAlBP: Mn(0.2)	4.75	4.39	0.293	0.7604	Present work
ZnAlBP: Mn(0.4)	4.62	4.24	0.286	0.7603	Present work
ZnAlBP: Mn(0.6)	4.48	4.11	0.256	0.7593	Present work
ZnAlBP: Mn(0.8)	4.26	3.94	0.239	0.7583	Present work
NaKB: Mn (5)	3.28	3.33	0.344	-----	11
LiPTB: Mn (0.5)	3.16	-----	0.27	0.5025	35
LiNaB: Mn (5)	3.10	-----	0.333	0.5108	43

The magnitude of band gaps was estimated by extrapolating the linear region of the plot towards the x-axis to intersect at $(\alpha h\nu)^2$ and $(\alpha h\nu)^{1/2} = 0$. The optical basicity, optical band gaps, and Urbach energies were calculated and are presented in table-4. The host ZnAlBP glass has maximum direct and indirect band gaps of 5.31 eV and 4.73 eV than Mn^{2+} doped ZnAlBP glasses. Both the energy gap values gradually decreased to 4.26 eV and 3.48 eV on increasing the Mn^{2+} concentration 0.2 % to 0.8 %. The structural changes, depolymerization, and availability of NBOs are might be responsible for the obtained variations in the energy gap. Urbach's energy is used to estimate the structural disorders in glassy materials.[38,39] The Urbach energy values are found to be decreased with an increase in Mn^{2+} concentration, indicating the decrease in localized states.[40]

Electron Paramagnetic Resonance Studies

The obtained EPR resonance signal in Mn^{2+} ions doped ZnAlBP glasses is due to the manganese ions entering into the host network as paramagnetic species. The EPR spectra of the prepared glasses showed a strong resonance signal with effective 'g' values at g≈1.98 and are shown in Fig.-6. The Mn^{2+} ion in the ground state with d^5 configuration is notable among other d^n configurations due to the existence of only one state with higher spin multiplicity ($^6S_{5/2}$). The present EPR spectra of all the concentrations of Mn^{2+} doped ZnAlBP glasses show a six line hyperfine structure (hfs) and shoulder signals at g ≅ 3.3 and g ≅ 4.3 were also identified.[41] "The resonance at g ≈ 1.98 is ascribed either may be because of isolated Mn^{2+} ions in octahedral symmetric sites slightly tetragonally distorted when the hyperfine structure (hfs) is resolved or associated ones". The Mn^{2+} ions participated in dipole-dipole or super exchange interactions, and is known to arise from the transition between the energy levels of the lower Kramer's doublet (± ½).[42] The well distinguished hyperfine structure (hfs) with g≈1.98, resonance clearlyshows that manganese ions are in symmetric sites (octahedral) and are isolated or notable different from each other. The sextet hyperfine splitting is the result of the interaction of electron spin with the Mn^{2+} nucleus, having spin I = 5/2. Several authors reported that the Mn^{2+} doped glasses are distinguished by an intense signal whose magnitude is nearer to the free electron value of g = 2.0023. In case of d^5 TM ions, "the axial distortion of octahedral symmetry gives rise to three doublets |± 5/2 >, |± 3/2 >, and |± 1/2 >, application of the Zeeman field remove the spin degeneracy of the Kramer's doublets". The obtained shoulder peaks at g≈3.3 and g≈4.3 are corresponding to rhombic surroundings of manganese ion. These peaks originates from transitions between the energy levels of the middle Kramer's doublets (|± 3/2 >) which are supposed to substitute the Zn^{2+} ion in the environment which is close to octahedral symmetry and is occurred from the transition between the energy levels of the lower doublet (|± 1/2 >).[43,44] The intensity variations in the resonance signals w.r.to manganese content is evidence for the existence of manganese ion in Mn^{2+} as well as Mn^{3+}state.

The two valence states of manganese ions that are available in glasses owing to the preparation process or the spin-spin interactions and optical spectra are evidence for the Mn^{3+} state. The calculated 'g' and 'A' values for the Mn^{2+} doped ZnAlBP glasses are given in Table-5. The g values are evaluated for all the

concentrations of Mn^{2+} doped ZnAlBP and it was noticed that the magnitude of g is independent of content which indicates the bonding nature. The negative shift in the g value w.r.to free electron g value (2.0023) indicates the predominant covalent nature. In the present study, the measured g and A values are evidence of the predominant ionic nature between Mn^{2+} and O^{2-} ions in the octahedral symmetry. The obtained A value of Mn^{2+} doped ZnAlBP glass is 90×10^{-4} T indicating Mn^{2+} ionic nature which is almost independent of alkali ion in the glass network. The magnitude of A is consistent with Mn^{2+} ions in octahedral coordination.[45]

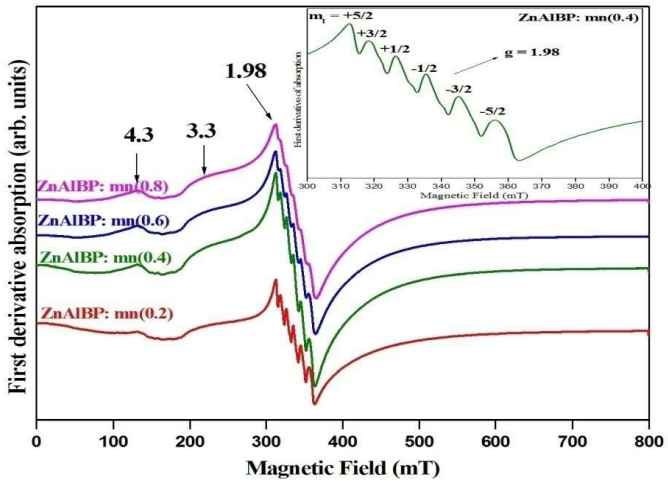

Fig.-6: EPR Spectra of Mn^{2+} Doped ZnAlBPGlass System

Table-5: Lande g-factor, Hyperfine Interaction Constant (A), Number of Spins (N), and Paramagnetic Susceptibility (χ)

Glass Sample	g-Factor	$A\times10^{-4}$ (cm^{-1})	$N\times10^{21}$	$\chi\times10^{-5}$ (m^3kg^{-1})	Ref.
ZnAlBP: Mn(0.2)	1.996	97.4	2.6199	6.428	Present work
ZnAlBP: Mn(0.4)	1.998	97.9	7.5484	18.559	Present wo
ZnAlBP: Mn(0.6)	1.998	89.3	4.7110	11.502	Present work
ZnAlBP: Mn(0.8)	1.996	89.3	6.5675	16.034	Present work
NaKB: Mn(5)	2.019	76.5	-----	-----	11
SrAlBSi: Mn(15)	2.035	89.6	-----	-----	15
LDS4G	1.98	-----	3.8	9.07	29
LiPTB: Mn(0.5)	2.0	-----	4.94	12.17	35
LiNaB: Mn (5)	1.995	83.1	10.4	-----	44

Calculation of the Population of Spin Levels (N)

The number of spins that participated in the resonance signal is estimated using the area under the curve of the EPR spectra with the reference ($CuSO_4.5H_2O$) concentration.[46] It is interesting to observe that the 'N' value increases up to 0.4 wt% from 0.2 wt% and thereafter, it decreases to 0.6 wt% and again it increases to 0.8 wt% however, the maximum value was obtained for ZnAlBP: Mn (0.4) glass.[44] The obtained non-linear trend of N with Mn^{2+}concentration is shown in Fig.-7.

Calculation of Paramagnetic Susceptibility (χ)

The magnetic susceptibility (χ) of the Mn^{2+} ion is determined using the standard formulae and the obtained values are well matched with the EPR data.[47] These results are very useful to know the distribution of dopant ions in the glass host and also the nature of the magnetic interactions among the ions in the selected compositions. The variation of magnetic susceptibility with selected Mn^{2+} concentration in ZnAlBP glass host is shown in Fig.-8.

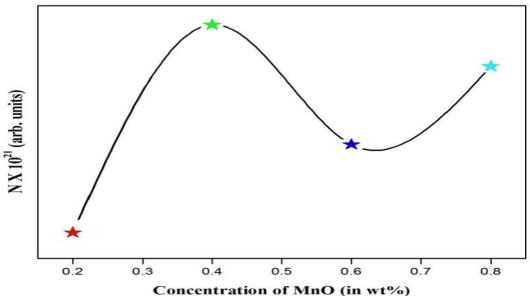

Fig.-7: Variation of Number of Spins (N) with MnO Concentration

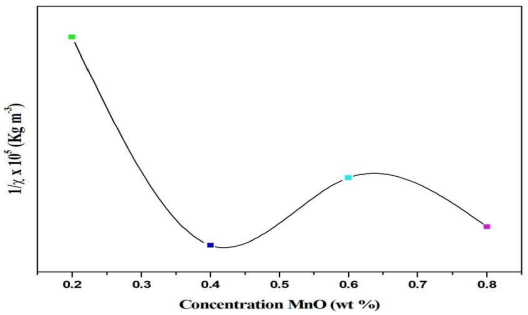

Fig.-8: Variation of Magnetic Susceptibility (χ) with MnO Concentration

CONCLUSION

The glassy nature of the ZnAlBP and Mn^{2+} doped ZnAlBP glasses was confirmed by XRD. The FT-IR results confirm the presence of BO_3 and BO_4 units with regular P-O-B and P-O-P bonds. The optical absorption spectra consist of optical transitions $^5E_g \rightarrow {}^5T_{2g}$, $^6A_{1g}(S) \rightarrow {}^4T_{2g}(G)$, and $^6A_{1g}(S) \rightarrow {}^4T_{1g}(G)$ at 480 nm, 526 nm, and 690 nm respectively due to d-d transitions of Mn^{2+} ions. The optical band gaps and Urbach energies are estimated, and the obtained trends are in good agreement with others reported for Mn^{2+} doped glassy materials. The EPR spectra of Mn^{2+} ions doped ZnAlBP glasses show a resonance signal at $g \approx 1.98$ with a well-resolved sextet hyperfine structure. The spin-Hamiltonian parameters ($g \approx 1.98$ and $A \approx 97.4$) are observed to be independent of Mn^{2+} ion concentration. The number of spins (N) and the paramagnetic susceptibility (χ) are calculated for Mn^{2+} ions in octahedral site symmetry and found to be maximum for ZnAlBP: Mn (0.4) glass.

ACKNOWLEDGMENT

One of the authors (J Suresh Krishna) expressed his gratitude to the UGC, the Government of India, for their financial support by awarding the Rajiv Gandhi National Fellowship (2016-17).

REFERENCES

1. M.H. Wan, P.S. Wong, R. Hussin, O. Hendrik, Lintang and SalasiahEndud, *Journal of Alloys Compounds*,**595**, 39(2014), https://doi.org/10.1016/j.optcom.2011.02.033
2. Hirokazu Masai, Yusuke Hino, Takayuki Yanagida and Yutaka Fujimoto, *Optical Materials*, **42**, 381(2015), https://doi.org/10.1016/j.optmat.2015.01.031
3. I. Ardelean, N. Muresan and P. Pascuta, *Materials Chemistry and Physics*, **101**, 177(2007), https://doi.org/10.1016/j.matchemphys.2006.03.010
4. N. Kiran, C.R. Kesavulu, A. Suresh Kumar and J.L. Rao, *Physica B: Condensed Matter*, **406**, 3816(2011), https://doi.org/10.1016/j.physb.2011.06.078
5. P. Venkat Reddy, C. LaxmiKanth, V.P. Rashanth Kumar, N. Veeraiah and P. Kistaiah, *Journal of Non-Crystalline Solids*, **351**, 3752(2005), https://doi.org/10.1016/j.jnoncrysol.2005.08.039
6. S. Hima Bindu, T. Rajavardhana Rao and Ch. Linga Raju, *Physica Scripta*, **90**, 065802(2015), https://doi.org/10.1088/0031-8949/90/6/065802

7. Doris Moncke, Efstratios I. Kamitsos, Andreas Herrmann, Doris Ehrt and Manfred Friedrich, *Journal of Non-Crystalline Solids*, **357**, 2542(2011), https://doi.org/10.1016/j.jnoncrysol.2011.02.017
8. I. Bratu, I. Ardelean, A. Barbu, V. Mih, D. Maniu and G. Botezan, *Journal of Molecular Structure*, **482**, 689(1999), https://doi.org/10.1016/S0022-2860(98)00940
9. A. Suneel Kumar, M.V. Sambasiva Rao, G. Chinna Ram and D. Krishna Rao, *Indian Journal of Physics*, **92**, 97(2018), https://doi.org/10.1007/s12648-017-1069-0
10. A. Radu, L. Baia, W. Kiefer and S. Simon, *Vibrational Spectroscopy*, **39**, 127(2005), https://doi.org/10.1016/j.vibspec.2005.01.004
11. R.P. Sreekanth Chakradhar, K.P. Ramesh, J.L. Rao and J. Ramakrishna, *Journal of Physics and Chemistry of Solids*, **64**, 641(2003), https://doi.org/10.1016/S0022-3697(02)00365-7
12. D. Toloman, L.M. Giurgiu and I. Ardelean, *Physica B: Condensed Matter*, **404**, 4198 (2009), https://doi.org/10.1016/j.physb.2009.07.187
13. I. Ardelean, M. Peteanu, S. Filip, V. Simon and I. Todor, *Solid State Communications*, **105,** 339(1998), https://doi.org/10.1016/S0038-1098(97)10056-4
14. A. Ramesh Babu, Ch. Rajya Sree, P.M. Vinaya Teja, S. Yusub and D. Krishna Rao, *Journal of Non-Crystalline Solids*, **358**, 131(2012), https://doi.org/10.1016/j.jnoncrysol.2012.03.012
15. A. Rupesh Kumar, T.G.V.M. Rao, N. Veeraiah and M. Rami Reddy, *Optical Materials*, **35**, 402(2013), https://doi.org/10.1016/j.optmat.2012.09.008
16. A.V. Ravi Kumar, Ch. Srinivasa Rao, N. Narasimha Rao,V. Ravi Kumar, I.V. Kityk and N. Veeraiah, *Journal of Non-Crystalline Solids*, **358**, 1278(2012), https://doi.org/10.1016/j.jnoncrysol.2012.02.032
17. D. Ehrt and W. Seebar, *Journal of Non-Crystalline Solids*, **129**, 19(1991), https://doi.org/10.1016/0022-3093(91)90076
18. G. E. El-Falaky and O.W. Guirguis, *Journal of Non-Crystalline Solids*, **358**, 1746(2012), https://doi.org/10.1016/j.jnoncrysol.2012.05.009
19. M. Rami Reddy, G. Naga Raju and N. Veeraiah, *Indian Journal of Engineering & Materials Sciences*, **13**, 426(2006)
20. I.E.C. Machado, L. Prado, L. Gomes, J.M. Prison and J.R. Martinelli, *Journal of Non-Crystalline Solids*,**348**, 113(2004), https://doi.org/10.1016/j.jnoncrysol.2004.08.135
21. D. Siva Raju, B. Deva Prasad Raju, S. Hima Bindu, M. Hema Latha, J. Suresh Krishna, V. Vinay Krishna and Ch. Linga Raju, *Materials Today: Proceedings*, **47(14)**, 4364(2021), https://doi.org/10.1016/j.matpr.2021.05.087
22. A.U. Ahamad, S. Hashim and S.K. Goshal, *Journal of Alloys Compounds*, **844**, 156(2020), https://doi.org/10.1016/j.jallcom.2020.156176
23. R. Vijay Kumar, G. Venkataiah and K. Marimuthu, *Journal of Alloys Compounds*, **652**, 234(2015), https://doi.org/10.1016/j.jallcom.2015.08.219
24. S. Hima Bindu, D. Siva Raju, V. Vinay Krishna, T. Rajavardhana Rao, K. Veera Brahmam and Ch. Linga Raju, *Optical Materials*, **62,** 655(2016), https://doi.org/10.1016/j.optmat.2016.10.055
25. P.Vijaya Lakshmi, T.G.V.M. Rao, K. Neeraja, D.V. Krishna Reddy and M. Rami Reddy, *Journal of Molecular Structure*, **1125**, 36(2016), https://doi.org/10.1016/j.molstruc.2016.06.064
26. G.N. Hemantha Kumar, J. Lakshmana Rao, N.O. Gopal, K.V. Narasimhulu, R.P.S. Chakradhar and A. Varada Rajulu, *Polymer*, **45**, 5407(2004), https://doi.org/10.1016/j.polymer.2004.05.068
27. A. Murali, R.P. Sreekanth Chakradhar and J. Lakshmana Rao, *Physica B: Condensed Matter*, **358,** 19(2005), https://doi.org/10.1016/j.physb.2004.12.021
28. C.R. Kesavulu, R.S. Muralidhara, J.L. Rao, R.V. Anavekar and R.P.S. Chakradhar, *Journal of Alloys Compounds*, **486**, 46(2009), https://doi.org/10.1016/j.jallcom.2009.07.040
29. A.R. Molla, R.P.S. Chakradhar, C.R. Kesavulu, J.L. Rao and S.K. Biswas, *Journal of Alloys Compounds*, **512**, 105(2012), https://doi.org/10.1016/j.jallcom.2011.09.031
30. C. Parthasaradhi Reddy, V. Naresh and K.T. Ramakrishna Reddy, *Optical Materials*, **51**, 154(2016), https://doi.org/10.1016/j.optmat.2015.11.035
31. B. Sumalatha, I. Omkaram, T. Rajavardhana Rao and Ch. Linga Raju, *Physica B: Condensed Matter*, **411**, 99(2013), https://doi.org/10.1016/j.physb.2012.11.021

32. Ch. Linga Raju, N.O. Gopal, K.V. Narasimhulu, J. Lakshmana Rao and B.C. Venkata Reddy, *Spectrochimica Acta Part A: Molecular and Biomolecular Spectroscopy*, **61**, 2181(2005), https://doi.org/10.1016/j.saa.2004.09.002
33. D. Siva Raju, S. Hima Bindu, J. Suresh Krishna, V. Vinay Krishna and Ch. Linga Raju, *Journal of Physics Conference Series*, **1913**, 012011(2021), https://doi:10.1088/1742-6596/1913/1/012011
34. M. A. Hassan and C. A. Hogarth, *Journal of Materials Science*, **23**, 2500(1988), https://doi.org/10.1007/BF01111908
35. R.P. Sreekanth Chakradhar, G. Sivaramaiah, J. Lakshmana Rao and N.O. Gopal, *Spectrochimica Acta Part A*, **62**, 761(2005), https://doi.org/10.1016/j.saa.2005.02.045
36. T. Rajavardhana Rao, I. Omkaram, B. Sumalatha, K. Veera Brahmam and Ch. Linga Raju, *Solid State Ionics*, **18**, 695(2012), https://doi.org/10.1007/s11581-012-0666-3
37. D. Siva Raju, Megala Rajesh, S. Hima Bindu, J. Suresh Krishna, V. Vinay Krishna, B. Deva Prasad Raju and Ch. Linga Raju, *Rasayan Journal of Chemistry*, **14(4)**, 2392(2021), http://doi.org/10.31788/RJC.2021.1446523
38. P.C. Taylor and P.J. Bray, *Journal of Physics and Chemistry of Solids*, **33**, 43(1972), https://doi.org/10.1016/S0022-3697(72)80053-2
39. Y.D. Siva Prasad, A. Veerabadra Rao, K. Srikanth and K.A. Emmanuel, *Rasayan Journal of Chemistry*, **4(2)**, 358(2011)
40. N.F, Mort and E.A. Davis, *Electron Processes in Non-Crystalline Materials*, Clarendon, Oxford, (1971), https://doi.org/10.1016/0040-6090(72)90068-5
41. V. Parvathi1, J. Sai Chandra , Y. Sunandamma and H.Ananda Lakshmi, *Rasayan Journal of Chemistry*, **13(1)**, 395(2020), http://dx.doi.org/10.31788/RJC.2020.1315197
42. P. Giri Prakash, A. Murali and J.L. Rao, *Modern Physics Letters*, **16**, 143(2002), https://doi.org/10.1142/S0217984902003634
43. Shiv Prakash Singh, R.P.S Chakradhar, L.L. Rao and Basudeb Karmakar, *Physica B Condens. Matter*, **405**, 2157(2010), https://doi.org/10.1016/j.physb.2010.01.123
44. Md. Ehasanulla, K. Srikanth, A. Veerabhadra Rao and K. A. Emmanuel, *Rasayan Journal of Chemistry*, **4(2)**, 343(2011)
45. R. P. Sreekanth Chakradhar, B. Yasoda, J.L. Rao and N.O. Gopal, *Journal of Non-Crystalline Solids*, **353**, 2355(2007), https://doi.org/10.1016/j.jnoncrysol.2007.04.002
46. P. Pascuta, M. Bosca, G. Borodi and E. Culea, *Journal of Alloys Compounds*, **509**, 4314(2011), https://doi.org/10.1016/j.jallcom.2011.01.056
47. R.M. Krishna, J.J. Andre, J.L. Rao and W.E. Antholine, *Materials Research Bulletin*, **34,** 1521(1999), https://doi.org/10.1016/S0025-5408(99)00182-8

[RJC-6992/2022]